

PERFORMANCE TEST OF THE NEXT GENERATION X-RAY BEAM POSITION MONITOR SYSTEM FOR THE APS UPGRADE*

B.X. Yang, Y. Jaski, S.H. Lee, F. Lenkszus, M. Ramanathan, N. Sereno, F. Westferro
Advanced Photon Source, Argonne National Laboratory, Argonne, IL 60439 USA

Abstract

The Advanced Photon Source is developing its next major upgrade (APS-U) based on the multi-bend achromat lattice. Improved beam stability is critical for the upgrade and will require keeping short-time beam angle change below $0.25 \mu\text{rad}$ and long-term angle drift below $0.6 \mu\text{rad}$. A reliable white x-ray beam diagnostic system in the front end will be a key part of the planned beam stabilization system. This system includes an x-ray beam position monitor (XBPM) based on x-ray fluorescence (XRF) from two specially designed GlidCop A-15 absorbers, a second XBPM using XRF photons from the Exit Mask, and two white beam intensity monitors using XRF from the photon shutter and Compton-scattered photons from the front end beryllium window or a retractable diamond film in windowless front ends. We present orbit stability data for the first XBPM used in the feedback control during user operations, as well as test data from the second XBPM and the intensity monitors. They demonstrate that the XBPM system meets APS-U beam stability requirements.

INTRODUCTION

The Advanced Photon Source (APS) storage ring will receive a major upgrade based on multi-bend achromat lattice [1]. The storage ring emittance will be under 70 pm-rad and the x-ray beam divergence will be dominated by the natural opening angle of the undulator radiation, as expected from a diffraction-limited source. The angular beam stability tolerance is chosen to be a fraction of the beam angular spread. For example, the long-term drift tolerance is $0.6 \mu\text{rad RMS}$. For an XBPM at 20 m from the source, this specification translates to an x-ray beam position tolerance of $12 \mu\text{m}$. We can assign 70% of this value, $8.5 \mu\text{m}$, to the XBPM's total error budget. Table 1 lists the XBPM tolerance for RMS AC beam motion ($0.01 - 1000 \text{ Hz}$) and long-term drift (7 days) derived in this manner from the beam stability specifications of the new storage ring.

The first XBPM system designed with these specifications were installed in Sector 27 of the APS storage ring in 2014 [2]. Figure 1 shows the XBPM system which includes the following components: (A) The first XBPM (XBPM1) measures the transverse x-ray beam positions at 18.6 m from the source, which is dominated by the angular motion of the e-beam; (B) the first intensity monitor (IM1) measures the beam intensity when the photon shutter (PS2) is closed; (C) the second XBPM (XBPM2) measures the x-ray beam position at the Exit Mask; and (D) the second intensity monitor (IM2) measures the beam intensity entering the user beamline. The two intensity monitors are used as alignment aids.

In this work, we will present the performance data of the XBPM1 in user operations, and discuss the design and performance of the XBPM2, IM1 and IM2.

Table 1: APS-U XBPM Tolerance ($Z = 20 \text{ m}$)

	Plane	AC motion	Long-term drift
X-ray beam position tolerance	X	$5.3 \mu\text{m}$	$12 \mu\text{m}$
	Y	$3.4 \mu\text{m}$	$10 \mu\text{m}$
Total XBPM error budget	X	$3.7 \mu\text{m}$	$8.5 \mu\text{m}$
	Y	$2.4 \mu\text{m}$	$7.1 \mu\text{m}$

GRID-XBPM PERFORMANCE

The first XBPM is a grazing-incidence insertion-device XBPM (GRID-XBPM) based on XRF from two GlidCop absorbers. Since it is sensitive only to hard x-rays, the bend magnet background is less than 3% of the XBPM signal at the maximum undulator gap (30 mm) or minimum undulator power ($K \sim 0.4$) for user operations. In the vertical plane, the XBPM calibration is independent of the undulator gap due to pinhole camera geometry used in x-ray readout optics. In the horizontal plane, the calibration is gap dependent but the offset is small due to symmetry in XBPM design [3,4].

Figure 2 shows the beam stability performance during user operations, as measured by the XBPM1. The data includes 60-days of operations in Summer 2015:

- In the week of June 30, only RFBPMs are used in the orbit feedback control and the x-ray beam is stabilized within $+10 \mu\text{m}$ and $-5 \mu\text{m}$ range, a reasonably good performance.
- After the July 4, the XBPM1 is added into the feedback loop. The black traces show 324-bunch mode of operations where the storage ring is filled twice daily. In these two weeks, we can see small saw tooth shape representing beam motion of $2 \mu\text{m}$ when the stored current decays from 102 mA to approximately 85 mA .
- After July 21, the blue trace shows operations in 24-bunch top-up mode, and the ring is filled every 2 – 3 minutes. The fuzzy traces represent the beam motion excited by the top-up shots. The severe reduction of the motion amplitude shows the effect of heavy filtering of the XBPM data in signal processing.
- When the XBPM is in the feedback loop, the x-ray beam motion is well within the boundary defined by the red and green lines, which represents the tolerance specifications in Table 1.
- No big jumps of beam positions are found in the gaps on Tuesday machine study days. This indicates that the XBPM helps the beam position return after studies, a feature important to beamline users.

* Work supported by U.S. Department of Energy, Office of Science, under Contract No. DE-AC02-06CH11357.

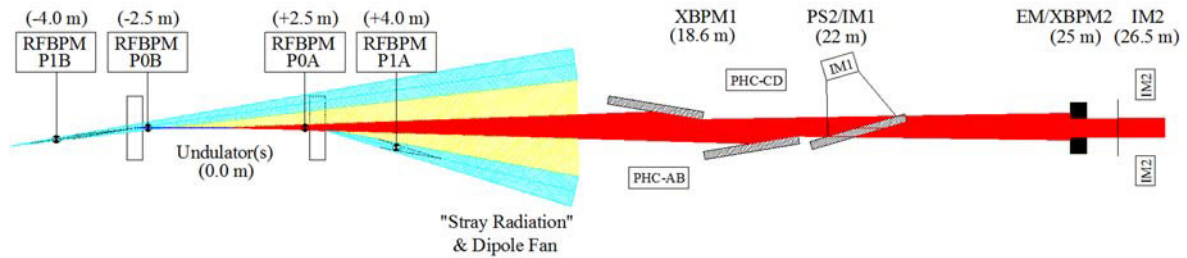


Figure 1: APS 27-ID RFBPM and XBPM system components for orbit controls.

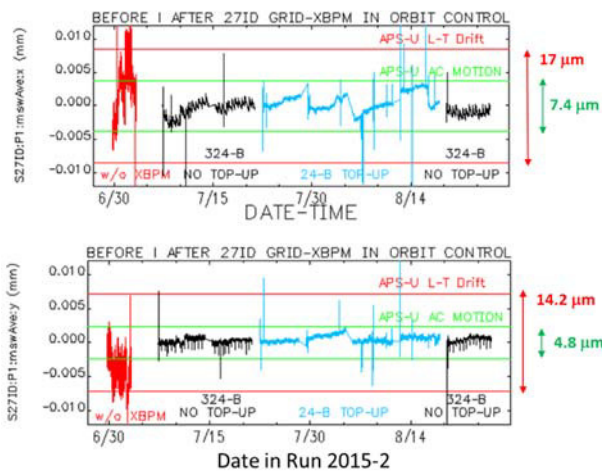


Figure 2: S27-ID GRID-XBPM data taken in 60-days of user operations: The upper panel is for the horizontal x-ray beam positions at 18.6 m from the undulator source and the lower panel is for the vertical beam positions.

SECOND X-RAY BPM

The second XBPM (XBPM2) derives its beam position information from the XRF from the front end Exit Mask (EM). Figure 3 shows its design: Two vertical apertures are placed at both sides of the EM entrance. Each aperture images the XRF photons from the opposite side onto two silicon PIN diodes located further upstream in the pumping chamber. If the beam moves down, more photons pass through aperture to reach the top PIN diode, and vice versa. The difference-over-sum of the two diode signal is proportional to the vertical beam position at the Mask. At the same time, the horizontal beam position can be derived from XRF intensities from two opposing sides of the Mask.

Since the horizontal aperture of the upstream XBPM1 is only 1.6 mm, only a small section of the Mask is illuminated by the beam during normal operations. If we use orbit control to hold beam position at the XBPM1, we can scan the orbit by changing set points of RFBPM PIB. Figure 4 shows the horizontal signal intensity ratio as a function of undulator gap for five different horizontal set points in PIB. Using the known geometry in Figure 1, we can calculate the x-ray beam positions at the Exit Mask, and calibrate the XBPM2.

Figure 5 shows the horizontal calibration constants and offsets for 27-ID XBPM2 as functions of undulator gap. The calibration constant is nearly gap independent. This is

likely due to the nearly constant size of the beam passing XBPM1, resulting a constant area of Exit Mask being exposed to the x-ray beam. The offset changes less than 5 μm over the entire undulator gap range. The change may come from the instrument error or from the source motion induced by undulator steering. Regardless of its origin, such a minute change is unlikely to be significant to user operations.

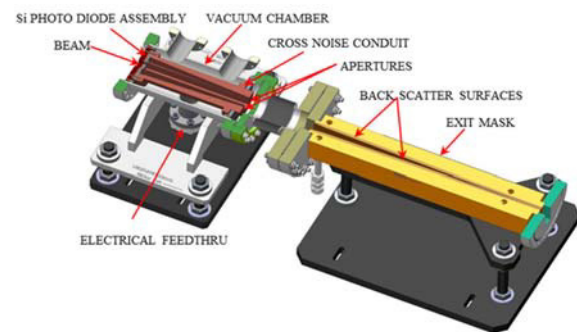


Figure 3: The second XBPM uses the XRF from the Exit Mask to monitor positions of the x-ray beam before it enters the beamline.

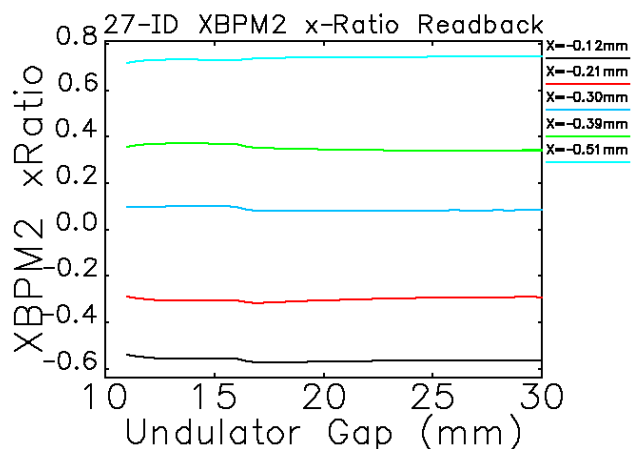


Figure 4: Vertical XBPM2 beam position signals (Δ/Σ) as functions of undulator gap for different x-ray beam positions on the Exit Mask.

FIRST INTENSITY MONITOR

The first intensity monitor (IM1) measures the XRF intensity from the photon shutter (PS2). Figure 6 shows the cross section of IM1. When the shutter is closed, it intercepts the beam on the outboard wall (upper right in the figure). The copper XRF photons will travel back upstream

through the imaging aperture and reach the silicon PIN diode. Since the length of shutter surface receiving the beam is long compared to the propagation distance, the XRF signal originating from an upstream point may be stronger than from the downstream point due to shorter distance to the diode. In order to get a signal truly proportional to XRF intensity and independent of beam spot location, the silicon PIN diode has a special mask shown in the inset of Fig. 6. The solid angle of the exposed detector surface is made independent of the beam spot position on the shutter.

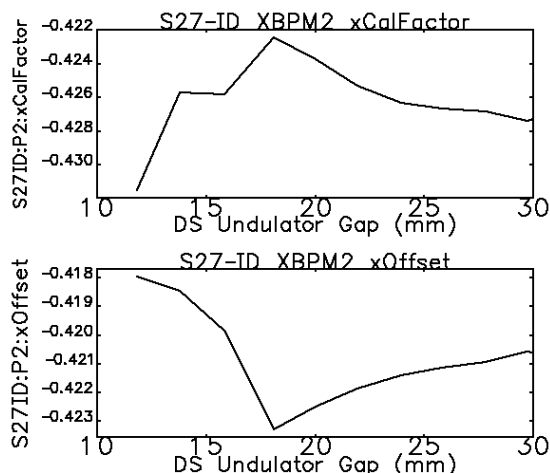


Figure 5: XBPM2 horizontal calibration constant (upper panel) and offset (lower panel) as functions of undulator gap.

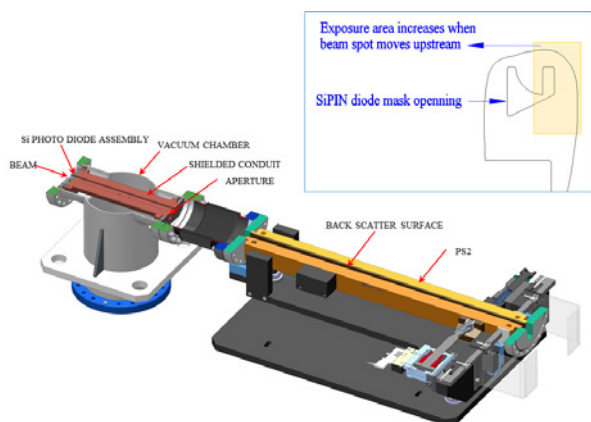


Figure 6: The first intensity monitor uses the XRF photons from the photon shutter (PS2) to monitors the beam intensity at the shutter.

Figure 7 shows the IM1 signal as functions of undulator gaps for upstream, downstream, and both undulators. We can see that two undulators generate the strongest signal and the upstream undulator the weakest one. For two 30-mm period undulator installed, the first harmonic reaches the copper K-edge near the gap of 16 mm, producing the spectral features in that region. Figure 8 shows the IM1 current as functions of horizontal x-ray beam position (projected to 20 m from source) for several undulator gap settings. For first harmonic well above copper K-edge, $G > 20$ mm, the horizontal profile has a well-defined single peak. After the first harmonic goes below the K-edge, the

profile starts to broaden into a flat top and eventually into a tweek peak shape. For longer period undulators such as U33, the maximum K may be as high as 2.85 and we will be able to see triple peaked profiles.

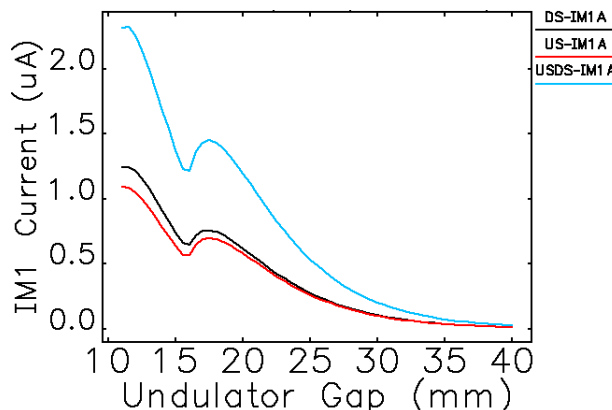


Figure 7: IM1 signal current as functions of the undulator gap for upstream (US), downstream (DS) and both undulators (USDS), respectively.

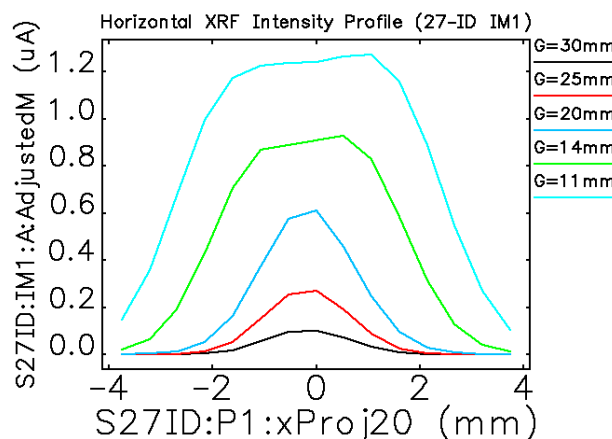


Figure 8: IM1 signal as functions of horizontal beam positions for selected undulator gaps.

SECOND INTENSITY MONITOR

For front ends with windows, the second intensity monitor (IM2) uses the front end Be window to intercept the beam [2]. For front ends without windows, IM2 uses a retractable, water-cooled diamond disc to intercept the beam. Figure 9 shows the windowless design in 27-ID.

Each IM2 can be used in two different modes. In Compton mode, the gold-plated photocathode facing the diamond film is biased negatively, its current signal is from the photoemission of the gold surface generated by (primarily Compton) scattered x-ray photons from the diamond disc. In photoemission mode, on the other hand, the gold-coated plate is biased positively to collect electrons in vacuum, its current is most likely derived from the photoemission from the diamond film.

Figure 10 compares the IM2 currents as functions of the undulator gap for different modes. Current from Compton mode is about three times higher than photoemission current, probably because the uncoated diamond film is not a

good photocathode. We choose Compton mode as our standard mode of operation.

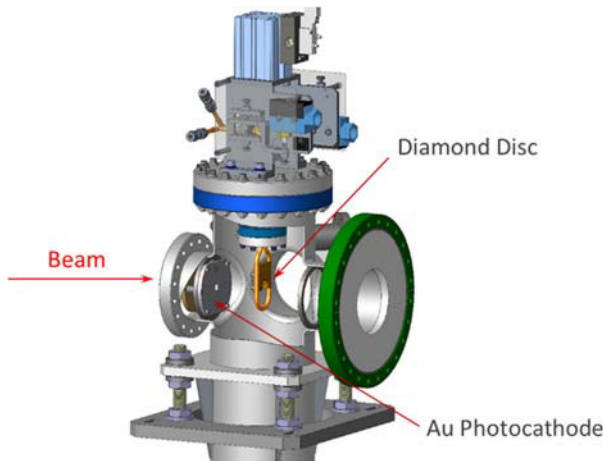


Figure 9: Cross section of IM2 for windowless front end.

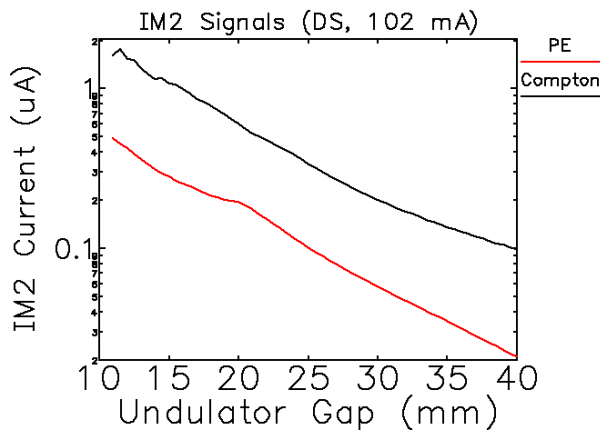


Figure 10: Absolute value of the IM2 current as functions of undulator gap for Compton and photoemission mode, respectively.

Figure 11 shows IM2 current for a horizontal beam angle scan for gap = 25 mm. This curve can be used for aligning white x-ray beam through two upstream apertures, a 1.6 mm horizontal gap for XBPM1 at 18.6 m, and 2 mm wide hole for the Exit Mask at 25 m. A deviation of ± 0.5 mm (20 μ rad) would result in approximately 6% changes in signal. For users seeking to align the beam to ± 10 μ rad accuracy, the IM2 signal level reduces only $\sim 1.5\%$ on each side. Users in 27-ID occasionally used this device for aligning the white x-ray beam or confirming proper operation of front end.

An ideal intensity monitor is expected to be independent of photon energies and insensitive to the undulator beam angle since the undulator spectrum depends on the angle from the beam axis. Figure 12 shows undulator gap scan data for five slightly different orbit angle settings. It shows that the IM2 spectra are very sensitive to beam angles in the gap region of 15 – 23 mm. This indicates that IM2 is quite sensitive to the x-ray energies and its data in 15 – 23 mm gaps range should be used with caution.

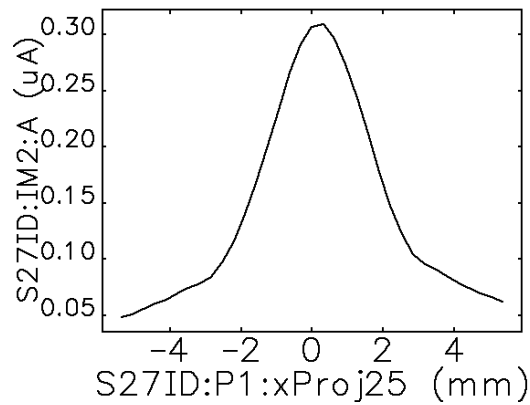


Figure 11: The normalized IM2 currents as functions of horizontal beam position for undulator gap of 25 mm.

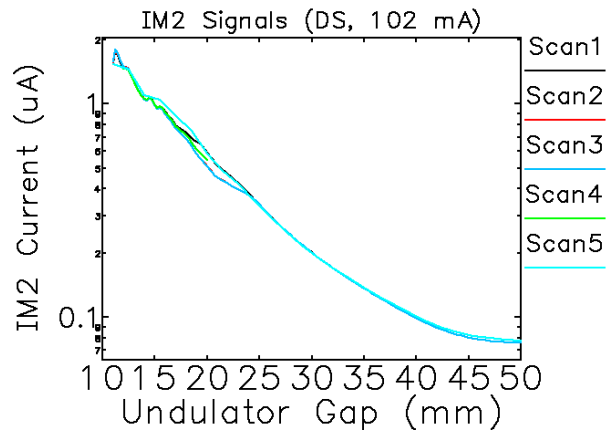


Figure 12: IM2 current as functions of undulator gap for five different small deviations in orbit angles.

CONCLUSION

The GRID-XBPM for in APS 27-ID high heat load front end showed that it has met the specifications for the APS Upgrade, with a possible long-term beam stability in the range of ± 3 μ m (± 120 nrad). In the horizontal plane, the second XBPM based on the Exit Mask has a gap-independent calibration and an insignificant gap-dependent offset. The first and the second intensity monitors (IM1 and IM2) are calibrated with undulator beam and used occasionally for beam alignment.

REFERENCES

- [1] M. Borland, V. Sajaev, Y. Sun, A. Xiao, Hybrid Seven-Bend-Achromat Lattice for the Advanced Photon Source Upgrade, IPAC 2015, pp. 1776 – 1779 (2015).
- [2] B.X. Yang, G. Decker, J. Downey, Y. Jaski, T. Kruey, S. H. Lee, M. Ramanathan and F. Westferro, Advanced x-ray beam position monitor system design at the APS, NAPAC 2013, pp. 1079 – 1081.
- [3] B. X. Yang, et al, High-power beam test of the APS grazing-incidence insertion device x-ray beam position monitor, BIW (2012), 235 – 237.
- [4] B. X. Yang, et al, Design and development for the next generation x-ray beam position monitor system at the APS, IPAC 2015, 1175 – 1177.